Sixth International Conference on Sustainable Construction Materials and Technologies. https://www.scmt-conferences.com/proceedings

HYDRATION PROPERTIES AND TECHNICAL BEHAVIOUR OF BLENDED BELITE CALCIUM SULFOALUMINATE CEMENTS

Antonio Telesca[1,2], Milena Marroccoli[1,2], Neluta Ibris[1,2], Frank Bullerjahn[3], Mohsen Ben Haha[4], Maciej Zajac[4]

[1]School of Engineering, Basilicata University, Viale dell'Ateneo Lucano 10, 85100 Potenza, Italy
[2]MATERIA Association, Via Libertà, 53, 85021 Avigliano (PZ), Italy
[3]Global R&D Heidelberg Materials AG, Zur Anneliese 7, 59320 Ennigerloh, Germany
[4]Global R&D Heidelberg Materials AG, Oberklamweg 2-4, 69181 Leimen, Germany
antonio.telesca@unibas.it; milena.marroccoli@unibas.it; neluta.ibris@unibas.it; frank.bullerjahn@heidelbergmaterials.com; maciej.zajac@heidelbergmaterials.com; mohsen.ben.haha@heidelbergmaterials.com

ABSTRACT

Belite calcium sulfoaluminate (BCSA) cements are environmentally friendly binders inasmuch as they can allow a significant reduction in CO_2 emissions thanks to the saving of both fuel consumption and limestone requirement. Compared to the production of ordinary Portland cement, the manufacture of BCSA cements is characterized by further relevant sustainable features, namely: (i) lower synthesis temperature (1250°-1350°C), (ii) easier clinker grindability and (iii) larger use of industrial wastes. Moreover, their environmental sustainability can be increased by the addition of supplementary cementitious materials.
The aim of this paper is to compare the hydration behaviour and the technical properties of a blast furnace slag (17.5% by mass) or a coal fly ash (17.5% by mass)-blended BCSA binder with a plain BCSA-system. All the binders, containing 2.5% by mass of slaked lime, were investigated by means of calorimetric, X-ray diffraction and differential thermal-thermogravimetric analyses, mercury intrusion porosimetry, expansion/shrinkage tests and mechanical compressive strength measurements.

Keywords
sustainability, belite calcium sulfoaluminate cement, supplementary cementitious materials, hydration, properties

INTRODUCTION

The cement industry is one of the main contributors to climate change because of greenhouse gas emissions, mainly carbon dioxide. In 2021, the global cement production was about 4.1 billion tonnes (CEMBUREAU, 2022), accounting for roughly 7% of all anthropogenic CO_2 emissions (IEA, 2022); consequently, the

search for a solution to reduce CO_2 emissions in the cement sector is urgently needed. In this regard, different levels of solutions were identified by the World Business Council for Sustainable Development in the "Technology Roadmap" (IEA, 2018), such as: (a) improving thermal and electric efficiency (GCCCA, 2021), (b) fostering the use of alternative fuels (Sahoo and Kumar, 2023), (c) stimulating the employment of capture and storage technologies to cement plants (Abanades et al., 2015; Benhelal et al., 201; Guo et al., 2024) and (d) developing low-CO_2 non-Portland binders (e.g., Mg-based binders, alkali-activated materials, calcium sulfoaluminate (CSA) and belite–CSA (BCSA) cements) (Marroccoli et al., 2010a; Schneider, 2019; Shi et al., 2019; Dung and Unluer, 2021; Walling and Provis, 2016; Capasso et al., 2021; Pol Segura et al., 2023; Ben Haha et al., 2019; Marroccoli et al., 2010b; Telesca et al., 2016, 2019; Chanunsali and Vaishnav, 2020). By the way, the manufacturing process of BCSA cements, compared to that of ordinary Portland cements (OPCs), is characterized by pronounced environmentally friendly features, such as: (I) lower synthesis temperature (usually 1250°-1350°C), (II) reduced amount of limestone requirement in the clinker generating raw mixture, (III) decreased specific fuel consumption and (IV) easier clinker grindability (Bullerjahn et al., 2014; Shenbagam and Chaunsali, 2022; Telesca et al., 2020; Zibret et al., 2022). BCSA cements represent a promising alternative to OPCs inasmuch as they exhibit similar technical properties, mostly depending on the ability of C_2S (dicalcium silicate) and $C_4A_3\$$ (ye'elimite) to produce, upon hydration, calcium silicate hydrates (CSH) and/or strätlingite (C_2ASH_8) as well as ettringite ($C_6A\$_3H_{32}$) (Alvarez Pinazo et al., 2016; Borštnara et al., 2020; Zajac et al., 2019). The sustainability of BCSA cements can be further increased through the addition of supplementary cementitious materials (SCMs) (Ma et al., 2014).

This paper compares the hydration behaviour and the technical properties of a blast furnace slag (BFS) or a coal fly ash (CFA)-blended BCSA binder (CB_S or CB_F, respectively) with a plain BCSA-system (CB_R). CB_S and CB_F contained 2.5% by mass of slaked lime (SL) and 17.5% by mass of BFS or CFA; CB_R included only 2.5% by mass of SL. The three cements were investigated by means of isothermal calorimetric, quantitative X-ray diffraction (QXRD) and differential thermal-thermogravimetric (DT-TG) analyses, mercury intrusion porosimetry (MIP), expansion/shrinkage (ES) as well as mechanical compressive strength tests.

EXPERIMENTAL

Materials

BCSA cement, CB (composed by BCSA clinker, CB_CLI, and 10% by mass of natural anhydrite), was supplied by HeidelbergCement AG. BFS, generated in a pig iron plant in South of ITALY, was finely pulverized in a laboratory planetary mill in order to pass through a 90 μm sieve; CFA was provided by an Italian coal power plant located in Puglia Region (ITALY). SL was type CL 90 (according to EN 459-1). CB_S and CB_F were prepared by mixing CB with BFS or CFA and SL (to stimulate the pozzolanic reaction of BFS and CFA).

The main oxides and the principal mineralogical phases of CB_CLI, BFS and CFA were respectively determined by X-ray fluorescence (XRF) and QXRD analyses.

Hydration procedure

Cement pastes were tested for curing periods ranging from 2 to 90 days. The cements were hydrated at room temperature by using a water/cement (w/c) ratio equal to 0.50. Cement pastes were cast into small plastic moulds (15-mm-high and 30-mm-diameter) and placed inside a thermostatic bath at 20°±2C°. At the end of each aging period the specimens were broken in half: one part was submitted to MIP measurements, the other was gently pulverized (grain size <63μm) for DT-TG and QXRD measurements. Both components, namely hardened fragments and fine powder, were treated with acetone (to stop hydration) and then left in a climatic chamber at 50°C for 60 minutes to remove the residual water; the samples were finally stored in a desiccator containing silica gel and soda lime (to ensure protection against H_2O and CO_2, respectively).

Cement pastes were also submitted to dimensional stability tests; in this regard, 18 prisms (15X15X78mm) were first cured in air at 20°C for 24 hours and then demolded. Tree prisms per each system were aged at 20°C under tap water; the remaining three samples were stored, at the same temperature, in a climatic chamber at 50% relative humidity. A length comparator apparatus was employed to measure the length of the samples at different aging period. The final length change was the average value resulting from the three different measurements.

Mortar prisms were prepared and stored according to the European Standard EN 196-1; compressive mechanical strength tests were carried out on samples cured from 2 to 90 days.

Characterization techniques

XRF analysis

XRF analysis was used to determine the chemical composition of the raw materials. A wave dispersive Bruker Explorer S4 apparatus (maximum power =1 kW; LiF200, PET, OVO-55, OVO-B as analyzing crystals) was used. Loss on ignition (l.o.i.) was determined according to EN 196-2.

Isothermal calorimetry

To investigate the hydration kinetics of the cement, paste samples were prepared with a w/c of 0.5. The paste samples for calorimetry measurements were prepared by external mixing for 30 seconds with 2500 rpm using a laboratory Vortex shaker (VF2, Janke and Kunkel Labortechnik). An isothermal conduction calorimeter (Thermometric TAM Air) was used to record the rate of the heat release during hydration for the first 7 days. The measurement was started directly after placing the samples in the calorimeter.

DT-TG analysis

A simultaneous DT-TG apparatus (NETZSCH-Tasc 414/3), operating between ambient temperature and 1000°C with a heating rate of 10°C min^{-1} in 150 μl alumina crucibles, was employed to evaluate cements hydration products. TG analysis was also used to quantitatively determine chemically bounded water at 650°C.

QXRD analysis

QXRD analyses were performed to determine the mineralogical composition for BFS, CFA, BC_CLI as well as the hydrated cement pastes. XRD analyses on BFS and CFA were carried out at Basilicata University on a Bruker D8 Advance diffractometer operating with a Cu Kα radiation generated at 40 kV and 40 mA. The patterns were performed in the 5°–60° 2θ range at a 0.02° 2θ step size and 10 seconds/step. QXRD analyses were carried out using Profex software, version 5.2.2 (Doebelin and Kleeberg, 2015), using the refinement strategy described in Döbelin et al. (2022).
The XRD patterns of BC_CLI and cement pastes were conducted at Heidelberg Materials laboratories using a Bruker D8 Advance in a θ-2θ configuration with a monochromatic CuKα radiation (λ = 1.54059 Å) and equipped with the LYNXEYE (1-d) detector. The generator settings were 40 kV and 40 mA. The measurement range was 5°-70° 2θ with a step-size of approximately 0.02° 2θ. Continuous rotation was applied during the data acquisition. For the quantitative analysis TOPAS 4.2 and the external standard method (D. Jansen, 2011) were employed.

MIP measurements

The porosity measurements were carried out by means of a Thermo-Finnigan Pascal 240 Series Mercury Porosimeter (maximum pressure, 200 MPa) equipped with a low-pressure unit (140 Series) able to generate a high vacuum level (10 Pa) and operate between 100 and 400 kPa.

RESULTS AND DISCUSSIONS

Table 1 shows the chemical and mineralogical composition for CB_CLI, BFS and CFA. From QXRD analysis, it can be easily argued that CB_CLI is mainly composed by C_2S (44.8% by mass) and $C_4A_3\$$ (38.3% by mass). Table 1 also indicates that CaO and SiO_2 are the main oxides for BFS, while Al_2O_3 and MgO can be considered as secondary components; its glassy content (evaluated by adding 10% mass of corundum as internal standard in each sample) is equal to 96% by mass. Moreover, from the chemical composition data, it is seen that CFA can be considered as a Class F fly ash, inasmuch as the silico-aluminous fraction prevails over the calcic one; QXRD analysis also revealed that the amorphous fraction for CFA is equal to 60% by mass as well as mullite and quartz represent the main crystalline phases.

Table 1. Chemical and mineralogical composition for CB_CLI, BFS and CFA, wt%

Chemical composition			
	CB_CLI	BFS	CFA
CaO	49.4	37.3	5.5
SiO_2	16.2	35.3	54.2
Al_2O_3	14.3	11.2	20.3
Fe_2O_3	2.2	1.0	5.3
MgO	0.7	10.8	0.7
SO_3	11.6	1.8	2.0
Others*	2.2	1.9	5.2
l.o.i.	2.7	0.7	4.4
Mineralogical phase composition			
$C_4A_3\$$	38.3	-	-
β-C_2S	44.8	-	-
C$	2.8	-	-
S_2A_3	-	-	17.6
S	-	-	14.5
Others**	14.1	3.6	7.9
X-ray amorphous	n.a.	96.4	60.0

K_2O, MnO, Na_2O, P_2O_5, TiO_2

***Bredigite, calcite, merwinite, perovskite, for CB_CLI, BFS and CFA*

Figures 1 and 2 displays the results of the isothermal calorimetry measurements for the three cements. It is worth noting that, the initial peak for CB_R exhibits the lowest heat flow, whereas the other systems show a notably higher heat flow during the first hour; this indicates that both blended cements display a higher initial reactivity than the plain BCSA cement. At longer curing times, CB_R shows the second and third maximum at about 5 and 9 hours, respectively; the second and the third maximum for CB_S and CB_F are at about 18 and 25 hours, respectively.

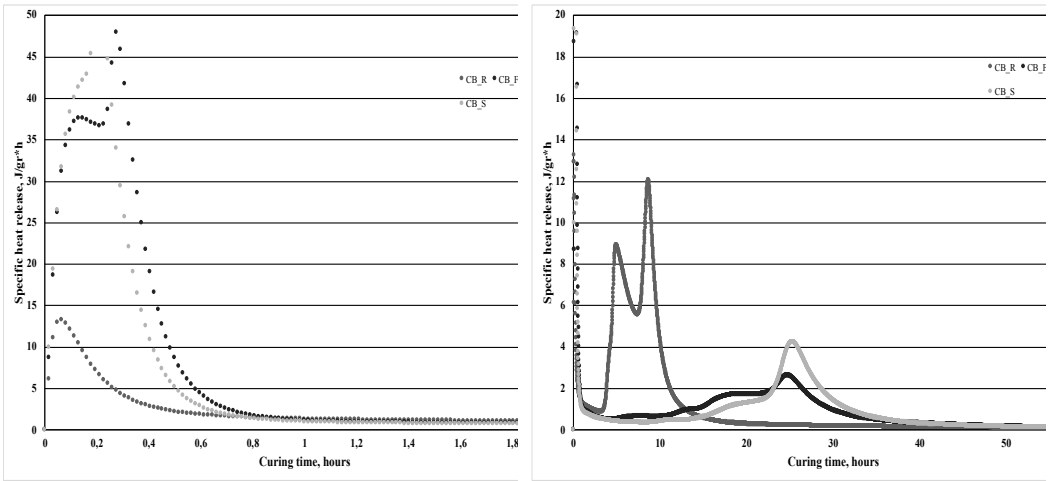

Figure 1. Hydration heat flow for the BCSA systems during the first 2 hours (left) and 60 hours (right) of hydration.

Moreover, CB_R shows the highest cumulative heat release after 7 days of hydration (about 260 J/g), whereas the heat of hydration of the other two cements is around 250 J/g.

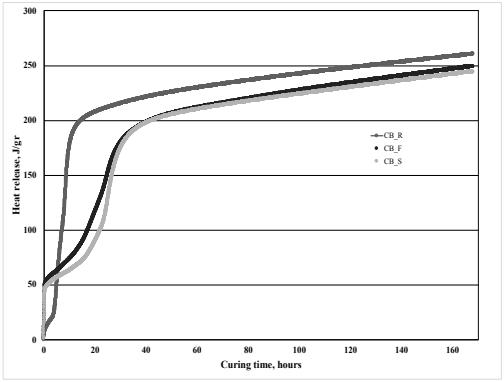

Figure 2. Development of heat of hydration for the three BCSA systems up to 168 hours of hydration.

In Figure 3 the DT-TG results for the three systems, cured from 2 to 90 days, are displayed.

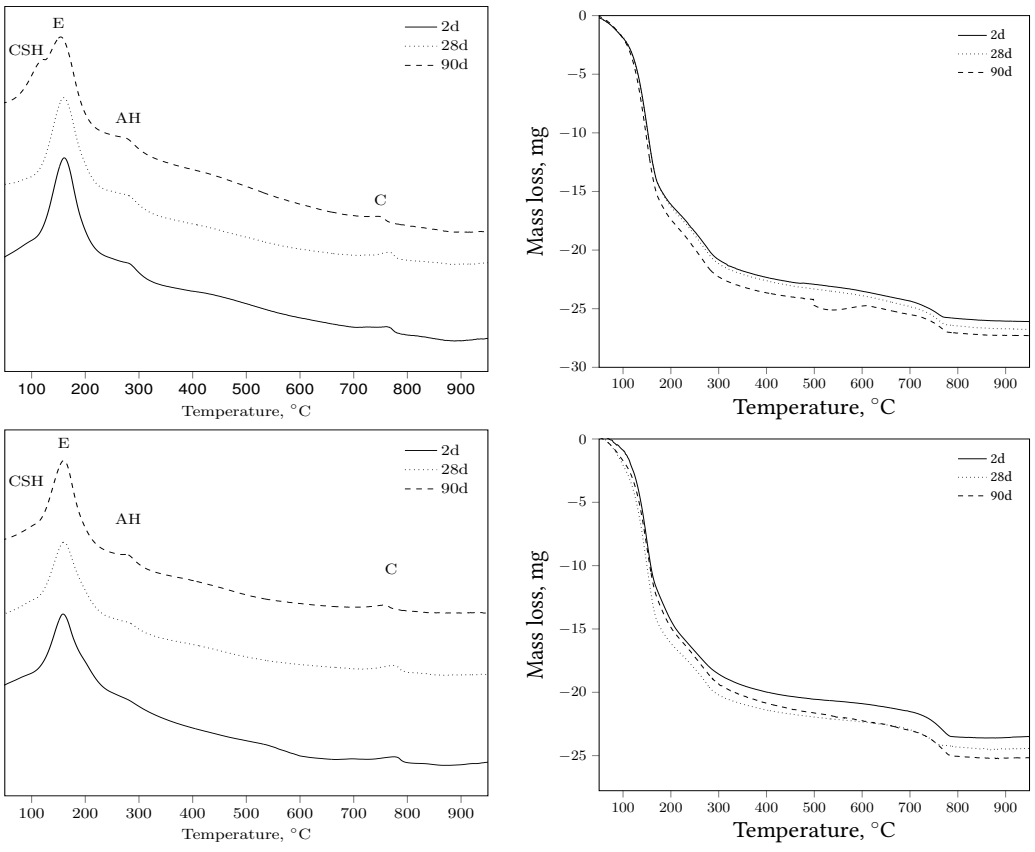

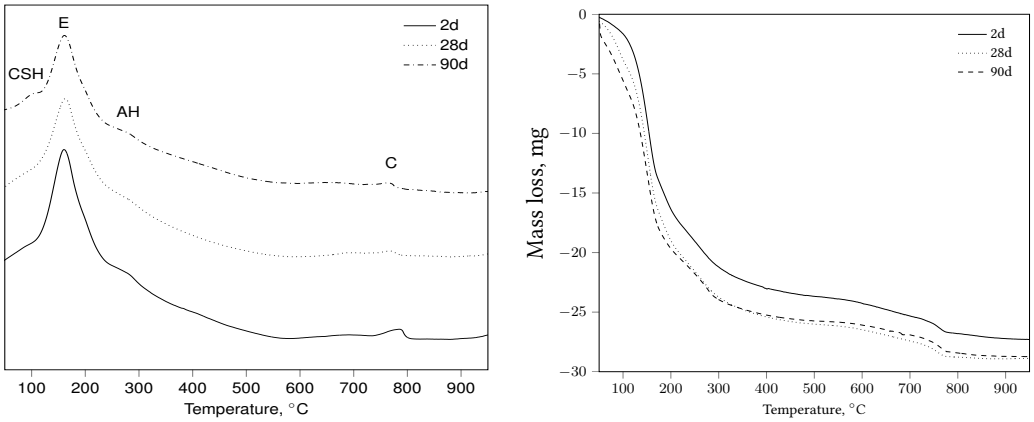

Figure 3. DT-TG thermograms for CB_R (up), CB_S (middle) and CB_F (down) cured at various ages. CSH=calcium silicate hydrates; E=ettringite; AH=aluminum hydroxide; C=calcium carbonate.

On the basis of the scientific literature data (Taylor, 1997), calcium silicate hydrates (104°±7°C), ettringite (160°±2°C), aluminium hydroxide (280°±3°C) and calcium carbonate (769°±10°C) were individuated in the order of increasing temperature of the related endothermal peaks. Furthermore, strätlingite could not be detected owing to overlaps of the E signals in the DT.

The composition of the hydrated systems was analyzed by XRD coupled with Rietveld analysis (QXRD); moreover, TG weight losses were also employed to refer the detected phases to the anhydrous cements. XRD patterns (for samples hydrated at 2, 28 and 90 days) are shown in Figure 4, where only the most significant phases are indicated. The absence of CSH and AH_3, among the crystalline phases detected, is due to their amorphous nature (Marroccoli et al., 2007). These analyses allowed to detect the consumption of reactants, the presence of inert phases and the development of hydration products. As for the DT thermograms, it has been found that as curing time increases, the peaks for ettringite and strätlingite increase; in particular, the presence of strätlingite was already evident in the CB_F system after two days of curing.

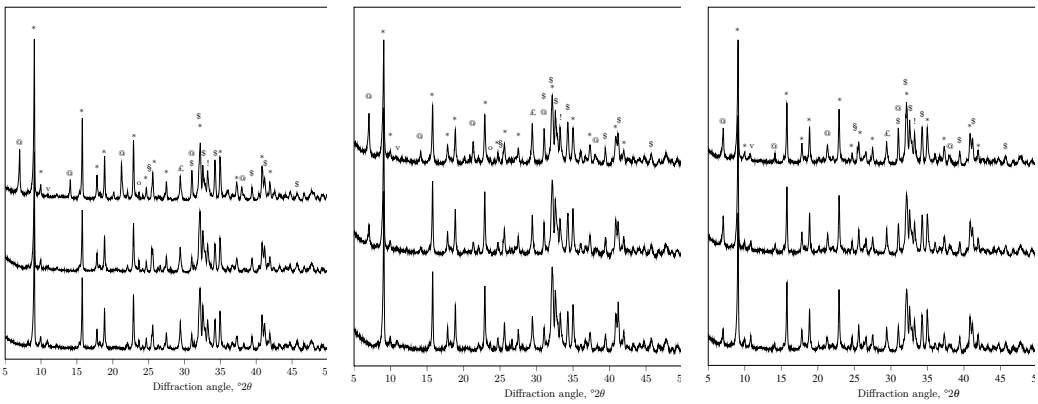

Figure 4: XRD patterns for CB_R (left), CB_S (middle) and CB_F (right) cured at various ages. @= strätlingite; *=ettringite; $=dicalcium silicate £=calcite; o=ye'elimite; v=hemicarboaluminate; §=anhydrite; !=tricalcium aluminate

The reached hydration degrees and the formed hydration products (Table 2) are the same in the three binders; conversely, the reaction kinetics and the hydrates contents are almost different. A slightly higher ye'elimite hydration degree (HD) was reached for both blended cements. Dicalcium silicate reacts initially faster in CB_F; however, CB_S reached the highest C_2S HD after 90 days of hydration.

Table 2. Hydration degree of main clinker phases and main hydration products, wt%.

	Hydration degree					
	CB _R	CB _R	CB _S	CB _S	CB _F	CB _F
Curing time, days	2	90	2	90	2	90
$C_4A_3\$$	95	97	99	99	99	98
β-C_2S	18	33	14	41	33	37
C$	84	91	96	96	93	95
C_4AF	100	100	100	100	100	100
	Hydration products					
	CB _R	CB _R	CB _S	CB _S	CB _F	CB _F
Curing time, days	2	90	2	90	2	90
$C_6A\$_3H_{32}$	35	44	29	28	36	37
C_2ASH_8	2	24	0	13	12	17
Amorphous	47	55	59	56	44	42

The ettringite contents are comparable, when accounting for the dilution effect, while strätlingite presents noticeable differences; in fact, its significant faster formation occurs in CB_F but similar contents (taking always into account the dilution effect) are reached after 90 days of hydration.

Figure 5 reports the trend of the dimensional stability in terms of E/S curves for CB_R, CB_S and CB_F up to 90 days of curing. The E and S curves show that the three binders differ very little from each other, above all when cured in air. Similarly to CB_R, when left in the air, the two blended cement pastes display a continuous and low shrinkage for about the first 30 days of curing; for the investigated systems, the maximum value of a steady shrinkage is compirised in the range of −0.13% (for CB_F) and −0.27% (for CB_R).

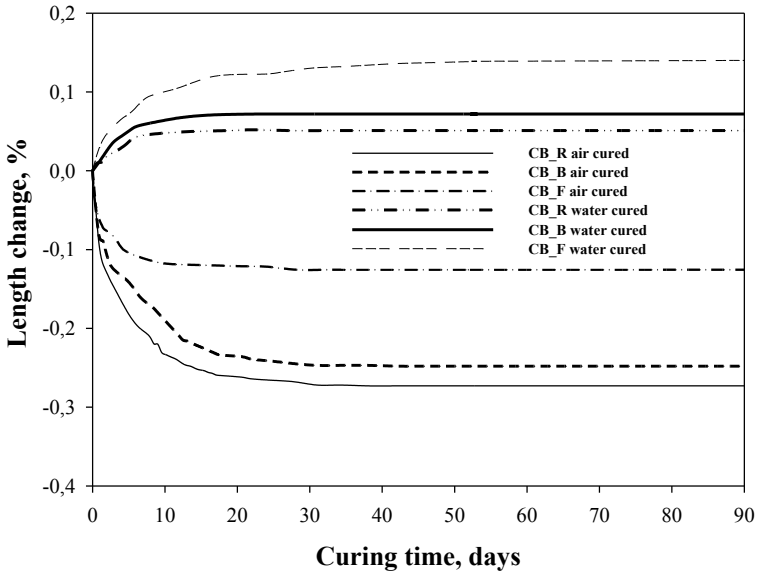

Figure 5. Dimensional stability curves for CB-based cements (air and water cured).

As far as the curing in water is concerned, the highest expansion values are achieved after about 40 days of hydration for CB_F, while only about 15 days for the other cements; on the whole the maximum expansion values are comprised in the range 0.05% (for CB_R) - 0.14% (for CB_F).

Cumulative and derivative Hg volume *vs* pore radius at various curing times for CB_R, CB_S and CB_F are shown in Figure 6. As expected, with the increase of curing time, the cumulative pore volume for the systems reduces; the cumulative pore volumes for CB_R passes from 160 mm^3/g (at 2 days) to 120 mm^3/g (at 90 days). At 2 days of curing, the cumulative pore volumes for BC_S and BC_F systems are slightly lower than that found for CB_R; this difference could be ascribed to the lower hydration rate of dicalcium silicate. Finally, after three months of hydration they result equal to 126 mm^3/g and 103 mm^3/g for CB_F and CB_S, namely 5% and 14% respectively higher and lower than that found CB_R. Furthermore, the three systems display a unimodal pore size distribution at the investigated curing periods; it has been found that, as curing time increases, the threshold pore radius decreases from about 120 nm to 70 nm for CB_R, from 150 nm to about 50 nm for CB_S and from 150 nm to 65 nm for CB_F.

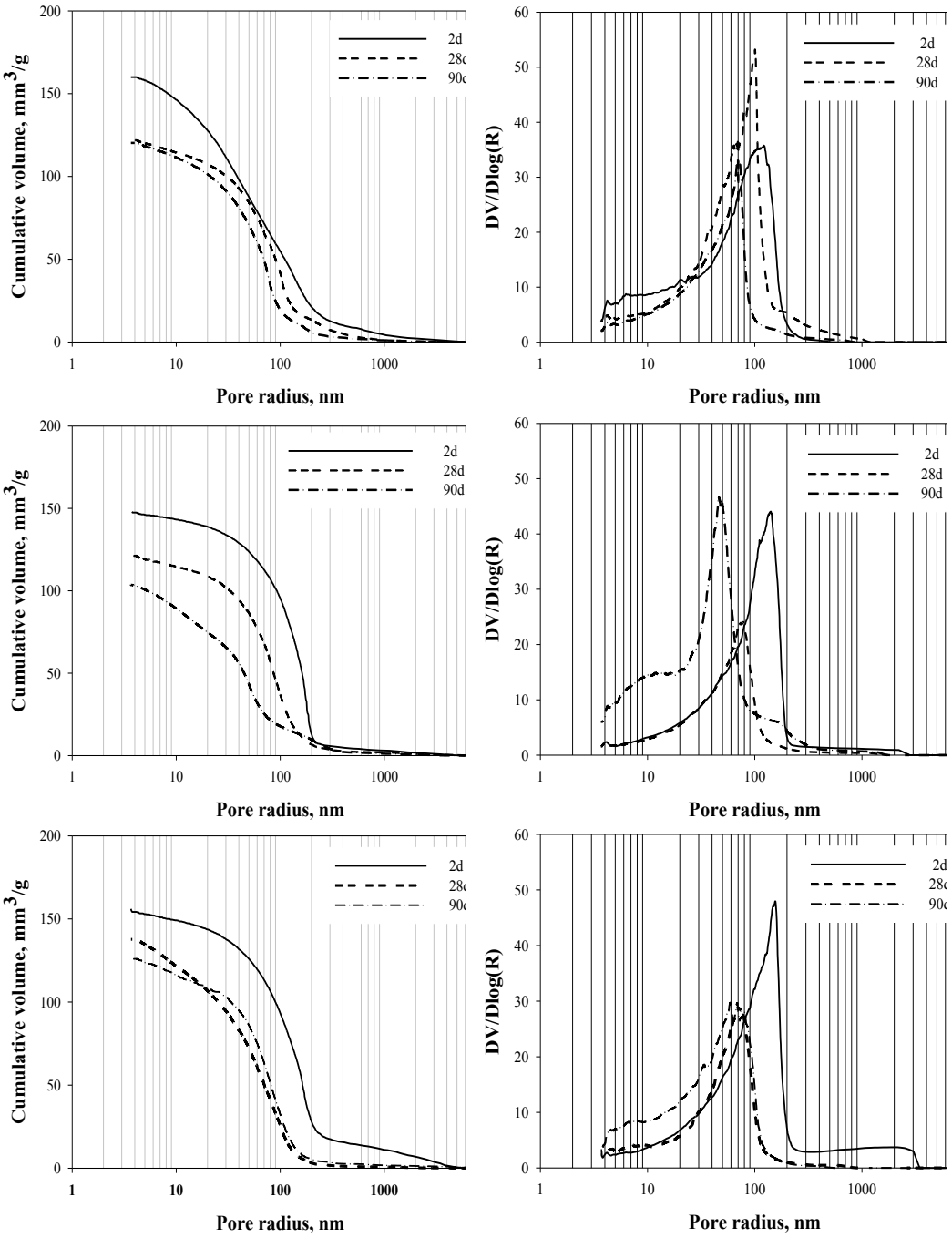

Figure 6: Cumulative (left) and derivative (right) Hg volume *vs.* pore radius for CB_R (up), CB_S (middle) and CB_F (down) cement pastes cured at 2, 28 and 90 days.

Figure 7 displays the total porosity (TP) values for the BCSA-based systems; the histograms clearly show a similar trend for all binders whose TP values decrease as curing time increases; at 2 days of hydration, the lowest TP value is exhibited by CB_R system due to the higher ye'elimite content. Finally, after 90 days of curing, the total porosity values for CB_R and CB_S (19.4% and 19.6%) respectively systems are almost the same and higher than that for CB_F (17.8%).

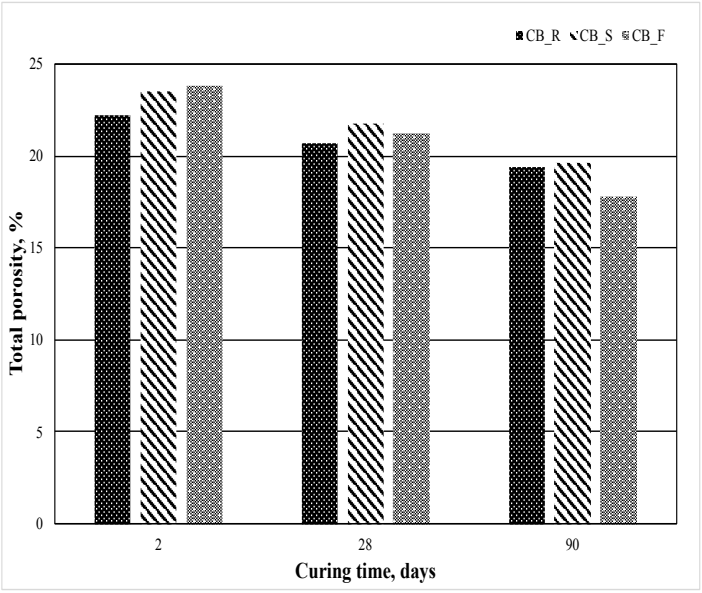

Figure 7. Total porosity values for CB_R, CB_S and CB_F pastes hydrated from 2 to 90 days.

Compressive strength measurements for CB-based mortars, as a function of the curing time, are reported in Figure 8. After 2 days of curing, the BCSA-blended mortars exhibited almost identical compressive mechanical strength values as the reference one.

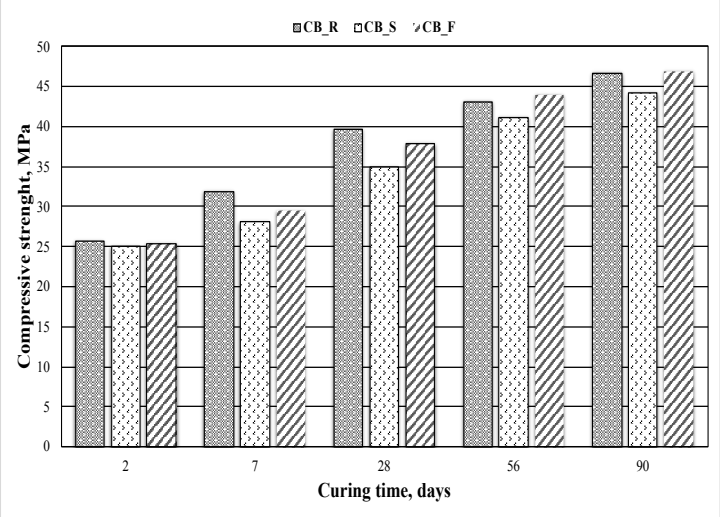

Figure 8. Results of compressive strength measurements for CB_R, CB_S and CB_F at 2, 7, 28, 56 and 90 days.

At 7 and 28 days the compressive strength values for CB_R are higher than those of the two blended cements (12% and 5% higher than those for CB_S and CB_F, respectively). Finally, after 56 and 90 days of curing, CB_R and CB_F-based mortars exhibit almost identical compressive mechanical strength values, resulting higher than those for CB_S.

CONCLUSIONS

This paper evaluates the possibility of using blast furnace slag (BFS) or pulverized coal fly ash (CFA) as alternative supplementary cementitious materials in belite calcium sulfoaluminate (BCSA)- blended cements; the utilization of BFS or CFA allows for the dilution of the BCSA cement, determining the subsequent environmental benefits, namely: (a) decreased CO_2 emissions; (b) energy saving per unit mass of cement; (c) reduction in natural resources extraction.
It has been found that the addition of 17.5wt% of BFS or CFA (together with 2.5% of slaked lime) to a BCSA cement can produce a binder with similar chemical, physical and technical characteristics.
Further investigations will deal with the use of other supplementary cementitious materials as well as with experimental investigations carried out for curing times longer than 3 months and involving also durability aspects.

REFERENCES

Abanades, J.C., Arias, B., Lyngfelt, A., Mattisson, T., and Brandani, S. (2015). "Emerging CO_2 capture systems". *Int. J. Greenh. Gas Control*, 40, 126–166.

Álvarez-Pinazo, G., Santacruz, I., Aranda, M.A.G., and De La Torre, Á.G. (2016). "Hydration of belite–ye'elimite–ferrite cements with different calcium sulfate sources". *Adv. Cem. Res.*, 28, 529–543.

Ben Haha, M., Winnefeld, F., and Pisch, A. (2019). "Advances in understanding ye'elimite-rich cements". *Cem. Concr. Res.,* 123, 105778.

Benhelal, E., Shamsaei, E., and Rashid, M.I. (2021). "Challenges against CO_2 abatement strategies in cement industry: A review". *J. Environ. Sci.,* 104, 84–101.

Borštnara, M., Daneuc, N., Dolenec, S. (2020). "Phase development and hydration kinetics of belite-calcium sulfoaluminate cements at different curing temperatures". *Cer. Int.,* 46, 29421–29428.

Bullerjahn, F., Schmitt, D., and Ben Haha, M. (2014). "Effect of raw mix design and clinkering process on the formation and mineralogical composition of (ternesite) belite calcium sulphoaluminate ferrite clinker". Ce*m. Concr. Res.,* 59, 87–95,

Capasso, I., Liguori, B., Ferone, C., Caputo, D., and Cioffi, R. (2021). "Strategies for the valorization of soil waste by geopolymer production: An overview". *J. Clean. Prod*., 288, 125646.

Cembureau. (2022). "Activity report 2022". *Cembureau, The European Cement Association*.

Chaunsali P., and Vaishnav K. (2020). "Calcium-Sulfoaluminate-Belite Cements: Opportunities and Challenge", *The Indian Concr. J.*, 94, 18–25.

Doebelin, N., and Kleeberg, R. (2015). "Profex: a graphical user interface for the Rietveld refinement program BGMN". *J. Appl. Crystallogr*., 48, 1573–1580.

Döbelin, N., Archer, R., and Tu, V. (2022). "A free and open-source solution for Rietveld refinement of XRD data from the CheMin instrument on board the Mars rover Curiosity". *Planet. Space Sci.,* 224, 105596.

Dung, N.T., and Unluer, C. (2021). "Advances in the hydration of reactive MgO cement blends incorporating different magnesium carbonates". *Constr. Build. Mater.,* 294, 123573.

GCCA (Global Cement and Concrete Association). (2021). The GCCA 2050 Cement and Concrete Industry Roadmap for Net Zero Concrete.

Guo, Y., Luo, L., Liu, T., Hao, L., Li, H., Liu, P., and Zhu, T. (2024). "A review of low-carbon technologies and projects for the global cement industry". *J. Env. Sci.,* 136, 682–697.

IEA. (2018). "Technology Roadmap: Low-Carbon Transition in the Cement Industry". International Energy Agency.

IEA. (2023). "Direct emissions intensity of cement production in the Net Zero Scenario, 2015-2030". *https://www.iea.org/data-and-statistics/charts/direct-emissions-intensity-of-cement-production-in-the-net-zero-scenario-2015-2030, 2022* (Last accessed November, 8, 2023).

Jansen, D. (2011) "The hydration of an Ordinary Portland Cement (OPC) and the influence of selected polymers: A mineralogical study using an external standard method for quantitative X-ray diffraction", Friedrich-Alexander-Universität Erlangen-Nürnberg (Dissertation).

Ma, B., Li, X., Shen, X., and Mao, Y. (2014). Huang, H. "Enhancing the addition of fly ash from thermal power plants in activated high belite sulfoaluminate cement". *Constr. Build. Mat.,* 52, 261–266.

Marroccoli, M. Nobili, M. Telesca, A., and Valenti, G.L. (2007). "Early hydration of calcium sulfoaluminate-based cement for structural applications" *Proc. Int. Conf. Sustain. Constr. Mater. Technol.,* Coventry, UK, 389–395.

Marroccoli, M., Montagnaro, F., Telesca, A., and Valenti, G.L. (2010a). "Environmental Implications of the Manufacture of Calcium Sulfoaluminate-Based Cements", *2nd Int. Conf. Sust. Constr. Mat. and Tech.*, Ancona (Italy), 625-635.

Marroccoli, M., Pace, M.L., Telesca, A., and Valenti, G.L. (2010b). "Synthesis of Calcium Sulfoaluminate Cements from Al_2O_3-Rich by-products from Aluminium Manufacture". *2nd Int. Conf. Sust. Constr. Mat. and Tech.*, Ancona (Italy), 615-623.

Pol Segura, I., Ranjbar, N., Juul Damø, A., Skaarup Jensen, L., Canut, M., and Arendt Jensen, P. (2023). "A review: Alkali-activated cement and concrete production technologies available in the industry". *Heliyon*, 9, E15718.

Sahoo, N., and Kumar, A. (2023). "Potential of solar thermal calciner technology for cement production in India and consequent carbon mitigation". *Proc. Saf. Env. Prot.,* 179, 667–676.

Schneider, M. (2019). "The cement industry on the way to a low-carbon future". *Cem. Concr. Res.*, 124, 105792.

Shenbagam, V.K., and Chaunsali, P. (2022). "Influence of calcium hydroxide and calcium sulfate on early-age properties of non-expansive calcium sulfoaluminate belite cement". *Cem. Concr. Comp.,* 128, 104444.

Shi, C., Qu, B., and Provis, J.L. (2019). "Recent progress in low-carbon binders". *Cem. Concr. Res.,* 122, 227–250.

Taylor, H.F.W. (1997). "Cement Chemistry". *Thomas Telford,* 2nd Edn.

Telesca A, Matschei T., and Marroccoli, M. (2020). "Study of Eco-Friendly Belite-Calcium Sulfoaluminate Cements Obtained from Special Wastes". *App. Sci.*, 10, 8650.

Telesca, A. Marroccoli, M. Tomasulo, M., Valenti, G.L., Dieter, H. and Montagnaro, F. (2016) "Low-CO_2 Cements from Fluidized Bed Process Wastes and Other Industrial By-Products". *Comb. Sci. Tech.*, 188, 492–503.

Telesca, A., Marroccoli, M., and Winnefeld, F. (2019). “Synthesis and characterisation of calcium sulfoaluminate cements produced by different chemical gypsums”. *Adv. Cem. Res.*, 31, 113–123.

Walling, S.A., and Provis, J.L. (2016). “Magnesia-Based Cements: A Journey of 150 Years, and Cements for the Future? ”. *Chem. Rev.*, 116, 4170–4204.

Zajac, M., Skocek, J., Stabler, C., Bullerjahn, F., and Ben Haha, M. (2019). “Hydration and performance evolution of belite–ye’elimite–ferrite cement”. *Adv. Cem. Res.,* 31, 124–137.

Zibret, L., Ipavec, A., and Dolenec, S. (2022). “Microstructural characteristics of belite–sulfoaluminate cement clinkers with bottom ash”. *Constr. Build. Mat.*, 321, 126289.